Evaluation of Electron Beam Deflections across a Solenoid Using Weber-Ritz and Maxwell-Lorentz Electrodynamics

Ray T. Smith, Fred P. M. Jjunju, and Simon Maher*

Abstract—The deflection of charged particle beams by electric and/or magnetic fields is invariably based on the field centred approach associated with Maxwell-Lorentz and incorporated into the Lorentz force formula. Here we present an alternative method of calculation based on the force formula of Weber-Ritz and which does not involve, directly, the field entities **E** and **B**. In this study we evaluate the deflection of an electron beam by a long solenoid carrying direct current and positioned centrally across the beam. The experiment has some bearing on the Aharonov-Bohm effect in that our calculations indicate that even for very long solenoids the classical force on the beam remains finite. The standard interpretation of the effect is, however, in terms of quantum mechanics and vector potential. Experimental measurements have been made of electron beam deflections by three solenoids, 0.25 m, 0.50 m and 0.75 m long; each solenoid is doubly wound with the same winding density (2600 turns per metre) and carrying the same current of 5.00 A d.c.. Our results indicate that, within the limits of experimental error, both Weber-Ritz and Maxwell-Lorentz theories correlate with measurements for the longer solenoids. However in the case of the shortest solenoid, the lack of uniformity of the magnetic field, leads to significant error in the calculation of beam deflection by the Lorentz force. By contrast in a Weber-Ritz calculation a precise value of beam deflection is obtained by equating the impulse of the non uniform beam force to the vertical momentum change of the electron. This is a fundamentally different approach which uses a statistical summation of forces on the beam in terms of relative velocities between moving electrons and involves a direct computation of the vertical force on the beam due to the circling solenoid current. This method has distinct advantages in terms of economy; that is, it does not involve directly field entities **E** and **B**, nor the leakage flux from the solenoid or the vector potential.

1. INTRODUCTION

The scientific paradigm which has dominated electromagnetic physics over the past hundred years is that of field theory as exemplified in the theories of Maxwell-Lorentz and later supplemented by Einstein's Special Relativity theory. In nearly all current texts the calculation of electron beam deflections is based on the law proposed by Lorentz over a century ago and given in terms of **E** (electric) and **B** (magnetic) field vectors as, $\mathbf{F} = e(\mathbf{E} + \mathbf{v} \times \mathbf{B})$, where **v** is the velocity of charge e with respect to the laboratory. However it is well established that such a linear law breaks down when applied to electron beams travelling at an appreciable fraction of light speed. Beam trajectories must then be corrected by the relativistic factor, γ, where $\gamma = (1 - \beta^2)^{-\frac{1}{2}}$ and $\beta = \frac{\mathbf{v}}{c}$. The justification for this correction is invariably ascribed to Special Relativity (Lorentz transformation) as predicting a mass increase with velocity ($m = m_0\gamma$). However, when the Lorentz force is contrasted with the older (and pre-Maxwellian) action at a distance theories of Weber or Ritz the question is posed as to which formulation is the more fundamental, Maxwell-Lorentz or Weber-Ritz?

Now regarding the Lorentz force law, we observe that while the force on a resting charge depends on **E**, the force on a moving charge is increased by a term corresponding to the law of Biot-Savart which was proven only for a closed neutral current. Lorentz himself remarked that, "*we now combine the two in the way shown in the equation, going beyond the direct results of experiment by the assumption that in general the two forces exist at the same time*" [1]. For such reasons O'Rahilly [1] has made the case that the Lorentz force law should not be regarded as fundamental. A more logical exposition is to be found in the older (pre-Maxwellian) action-at-a-distance theories associated with Gauss, Weber and Ritz. Such theories are concerned only with electrical forces between moving charges in relative motion. A brief survey of such action-at-a-distance theories is now given.

2. WEBER-RITZ: ACTION-AT-A-DISTANCE TYPE THEORIES

Weber-Ritz theories have an essential underlying simplicity. All electromagnetic actions are subsumed under a single force formula between moving charges. The force is logically assumed to depend on the simultaneous distance (r) between the charges, their relative velocity ($\dot{r}$) and relative acceleration ($\ddot{r}$). The relative velocity terms describe forces between current carrying conductors and magnets including motional electromagnetic induction while acceleration terms relate to transformer induction [2]. Moreover the force formula reduces to Coulomb's law for charges at rest. In general any force calculation involves a numerical computation of elemental forces between statistical aggregates of moving charge using Newtonian mechanics and the principle of superposition.

From an historical perspective Wilhelm Weber, as early as 1848, had proposed a second order force formula giving the force between electrical charges, e, e' in terms of their relative velocity and accelerations, as

$$F_r = \frac{ee'}{4\pi\varepsilon_0} \frac{\hat{\mathbf{r}}}{r^2} \left[1 + \frac{r\ddot{\mathbf{r}}}{c^2} - \frac{\dot{\mathbf{r}}^2}{2c^2} \right] \tag{1}$$

where F_r is the force along r, and $\hat{\mathbf{r}}$ is a unit vector along r. Some 50 years later (1908) Walther Ritz developed an emission theory of electromagnetic action which resulted in formulae very similar to those of Weber. In a modern context the work of Weber has undergone considerable development by Assis [3–6] while that of Ritz has received extensive coverage in O'Rahilly's work [1]. The theories of Weber and Ritz are largely unknown or ignored. Often this is due in part to misinformation that such theories are incorrect because they do not allow the derivation of Maxwell's equations. However, a careful reading of [1] or [3] would show that such a view is incorrect as summarised in [7].

Starting from Weber's force (Eq. (1)) and following O'Rahilly [1, Page 525], if **v** and **v'** are the velocities of charges e and e' distance r apart, and v_r, v'_r the respective velocities along r, then the relative velocity, u_r, along r is given as, $u_r = \frac{dr}{dt} = v_r - v'_r$. Also, $\frac{d^2r}{dt^2} = \frac{d}{dt} \sum (v_x - v'_x)(x - x')/r = (u^2 - u_r^2)/r + (f_r - f'_r)$, where u is the actual relative velocity between e and e', and $(f_r - f'_r)$ the relative acceleration along r. So Weber's force formula is now expressed in terms of relative velocities and accelerations as,

$$F_r(W) = \frac{ee'}{4\pi\varepsilon_0} \frac{\hat{\mathbf{r}}}{r^2} \left[1 + \frac{u^2}{c^2} - \frac{3u_r^2}{c^2} + \frac{r(f_r - f'_r)}{c^2} \right] \tag{2}$$

By contrast O'Rahilly [1, Page 520] gives Ritz's formula, based on the emission theory, as

$$F_r(R) = \frac{ee'}{4\pi\varepsilon_0 r^2} \left[\left(1 + \frac{(3-\lambda)}{4} \frac{u^2}{c^2} - \frac{3(1-\lambda)}{4} \frac{u_r^2}{c^2} + \frac{r(f_r - f'_r)}{c^2} \right) \hat{\mathbf{r}} - \frac{(1+\lambda)}{2} \frac{uu_r}{c^2} + \frac{rf_r}{2c^2} \right] \tag{3}$$

Note that in the Ritz formulation λ is a dimensionless constant whose value is determined according to the experimental data. When acceleration terms are ignored and $\lambda = -1$, the Weber and Ritz formula are the same. It is therefore appropriate to base our initial investigation on the Weber formula,

$$F_r(W) = \frac{ee'}{4\pi\varepsilon_0} \frac{\hat{\mathbf{r}}}{r^2} \left[1 + \frac{u^2}{c^2} - \frac{3u_r^2}{2c^2} \right] \tag{4}$$

The formula is now applied to the case of an electron beam crossing the central plane of a long solenoid carrying direct current.

3. FORCE ON AN ELECTRON BEAM TRAVERSING A LONG CURRENT CARRYING SOLENOID

3.1. Calculation for Single Current Loop

In Figure 1 a circular current loop, radius a, is located at the origin of a Cartesian system of coordinates $O(x, y, z)$. Q is a point on the loop containing a line element $a\delta\theta$, v' is electron drift velocity for a steady loop current, I, where $I = nAv'e$ and n is free electron density, A is cross sectional area of conductor and e is electron charge. An electron beam, speed v is directed parallel to the x axis and P is a typical point on the beam, coordinates (b, h, z). The force δF_r along r is now calculated between charges e' at Q where $e' = nA(a\delta\theta)e$ and e located at P, based on the Weber-Ritz force of Eq. (4). Then using $(\delta F_r) \cos\beta$ the elemental force $(\delta F)_y$ at right angles to the beam (i.e., parallel to the y axis) is obtained. Integration around the loop then gives the force on the electron at P.

The angles involved in the calculation are indicated in Figure 1 as θ, α, β, and γ, where:

θ is the angle between OQ and the x axis,

α is the angle between $r = \overrightarrow{QP}$ and x axis (v direction) where, $\cos\alpha = (b - a\cos\theta)/r$,

β is the angle between $r = \overrightarrow{QP}$ and y axis where, $\cos\beta = (h - a\sin\theta)/r$,

γ is the angle between $\overrightarrow{QT} = v'$ and the vector $\overrightarrow{QP} = r$ where, $\cos\gamma = (b\sin\theta - h\cos\theta)/r$, and, $r^2 = a^2 + b^2 + h^2 + z^2 - 2ab\cos\theta - 2ah\sin\theta$.

Recall that the Weber-Ritz force formula between point charges e and e' moving relative to one another being distance r apart is (Eq. (4)),

$$\delta F_r\,(W/R) = \frac{ee'}{4\pi\varepsilon_0}\frac{\hat{\mathbf{r}}}{r^2}\left[1 + \frac{u^2}{c^2} - \frac{3}{2}\frac{u_r^2}{c^2}\right]$$

where $\hat{\mathbf{r}}$ is a unit vector along r, u is the relative velocity between e velocity, v, and e' velocity, v', u_r is the relative velocity between e and e' along r. This gives,

$$u = v - v'\sin\theta$$

and since $v' \ll v$, $u^2 = v^2 - 2vv'\sin\theta$.

Also, $u_r = v\cos\alpha - v'\cos\gamma$ and, $u_r^2 = v^2\cos^2\alpha - 2vv'\cos\alpha\cos\gamma$ $(v' \ll v)$.
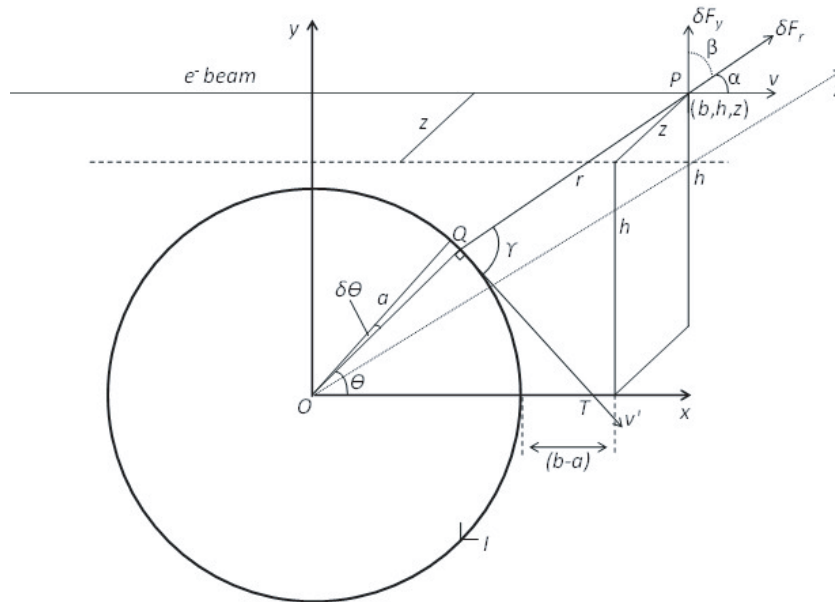

Figure 1. Geometry of circular current carrying loop at the origin of co-ordinates in the x-y plane and an electron travelling parallel to the x axis with velocity, v.

So the elemental force between e and e' along r is,

$$\delta F_{r-} = \frac{ee'}{4\pi\varepsilon_0} \frac{\hat{\mathbf{r}}}{r^2} \left[1 + \frac{(v^2 - 2vv'\sin\theta)}{c^2} - \frac{3}{2c^2}\left(v^2\cos^2\alpha - 2vv'\cos\alpha\cos\gamma \right) \right]$$

$$= \frac{ee'}{4\pi\varepsilon_0} \frac{\hat{\mathbf{r}}}{r^2} \left[1 + \frac{v^2}{c^2}\left(1 - \frac{3}{2}\cos^2\alpha \right) + \frac{vv'}{c^2}\left(2\sin\theta + 3\cos\alpha\cos\gamma \right) \right]$$

Now e is also subjected to an opposite force due to the stationary positive ions located at Q. Setting $v' = 0$ the force is,

$$\delta F_{r+} = \frac{ee'}{4\pi\varepsilon_0} \frac{\hat{\mathbf{r}}}{r^2} \left[1 + \frac{v^2}{c^2}\left(1 - \frac{3}{2}\cos^2\alpha \right) \right]$$

So the net force along r between the electron and the electron current is,

$$\delta F_r = \frac{ee'}{4\pi\varepsilon_0} \frac{\hat{\mathbf{r}}}{r^2} \left[\frac{vv'}{c^2}\left(3\cos\alpha\cos\gamma - 2\sin\theta \right) \right]$$

So the net deflective force at right angles to the beam (i.e., in the y direction) is then, $(\delta F)_y = \delta F_r \cos\beta$ giving,

$$(\delta F)_y = \frac{ee'vv'}{4\pi\varepsilon_0 c^2} \frac{\hat{\mathbf{r}}}{r^2} \left[3\cos\alpha\cos\beta\cos\gamma - 2\sin\theta\cos\beta \right]$$

Now, $e' = (nAea\delta\theta)$ and $I = nAv'e$ so,

$$\frac{ee'vv'\hat{\mathbf{r}}}{4\pi\varepsilon_0 c^2 r^2} = \frac{e\left(nAea\delta\theta \right)vv'}{4\pi\varepsilon_0 c^2} \frac{\hat{\mathbf{r}}}{r^2} = \frac{evIa\delta\theta}{4\pi\varepsilon_0 c^2} \frac{\hat{\mathbf{r}}}{r^2}$$

Making,

$$(\delta F)_y = \frac{evI}{4\pi\varepsilon_0 c^2} \left[\frac{3a\left(b - a\cos\theta \right)\left(h - a\sin\theta \right)\left(b\sin\theta - h\cos\theta \right)}{r^5} - \frac{2a\sin\theta\left(h - a\sin\theta \right)}{r^3} \right] d\theta$$

The force due to the complete loop is then,

$$(F)_y = \frac{evI}{4\pi\varepsilon_0 c^2} \left[-2ah \int_0^{2\pi} \frac{\sin\theta}{r^3}d\theta + 2a^2 \int_0^{2\pi} \frac{\sin^2\theta}{r^3}d\theta + 3ab^2 h \int_0^{2\pi} \frac{\sin\theta}{r^5}d\theta - 3a^2 b^2 \int_0^{2\pi} \frac{\sin^2\theta}{r^5}d\theta \right.$$

$$\left. -3a^3 h \int_0^{2\pi} \frac{\sin\theta\cos^2\theta}{r^5}d\theta - 3abh^2 \int_0^{2\pi} \frac{\cos\theta}{r^5}d\theta + 3a^2 h^2 \int_0^{2\pi} \frac{\cos^2\theta}{r^5}d\theta + 3a^3 b \int_0^{2\pi} \frac{\sin^2\theta\cos\theta}{r^5}d\theta \right]$$

So finally the force on the e *beam* located at point (b, h, z), due to the single current loop and acting in the y direction is,

$$(F_r)_y = \frac{evI}{4\pi\varepsilon_0 c^2} \left[-2ah\,[I_1] + 2a^2\,[I_2] + 3ab^2 h\,[I_3] - 3a^2 b^2\,[I_4] - 3a^3 h\,[I_5] - 3abh^2\,[I_6] + 3a^2 h^2\,[I_7] + 3a^3 b\,[I_8] \right] \quad (5)$$

where, $[I_1] = \int_0^{2\pi} \frac{\sin\theta}{r^3}d\theta$; $[I_2] = \int_0^{2\pi} \frac{\sin^2\theta}{r^3}d\theta$; $[I_3] = \int_0^{2\pi} \frac{\sin\theta}{r^5}d\theta$; $[I_4] = \int_0^{2\pi} \frac{\sin^2\theta}{r^5}d\theta$; $[I_5] = \int_0^{2\pi} \frac{\sin\theta\cos^2\theta}{r^5}d\theta$; $[I_6] = \int_0^{2\pi} \frac{\cos\theta}{r^5}d\theta$; $[I_7] = \int_0^{2\pi} \frac{\cos^2\theta}{r^5}d\theta$; $[I_8] = \int_0^{2\pi} \frac{\sin^2\theta\cos\theta}{r^5}dj$ and $r = (a^2 + b^2 + h^2 + z^2 - 2ab\cos\theta - 2ah\sin\theta)^{1/2}$.

The final stage of the calculation is then to evaluate the force at various points along the electron beam due to the complete solenoid. This is now considered.

3.2. Calculation Based on Solenoid as Stack of Current Loops

The use of a standard spherical beam tube (Teltron) in the present investigation places restrictions on the location of the current carrying solenoid in relation to the electron beam. Our calculation is then based on the solenoid located above and to one side of the beam as illustrated in Figure 2; the beam is then in the central (x, y) plane of the solenoid.

The solenoid radius a, and distance h of the beam below the x axis are fixed. The x coordinate, $-b$, is variable between 0 and $-0.1\,\text{m}$ in steps of $-0.002\,\text{m}$. This enables calculation of the force $F_y(b)$
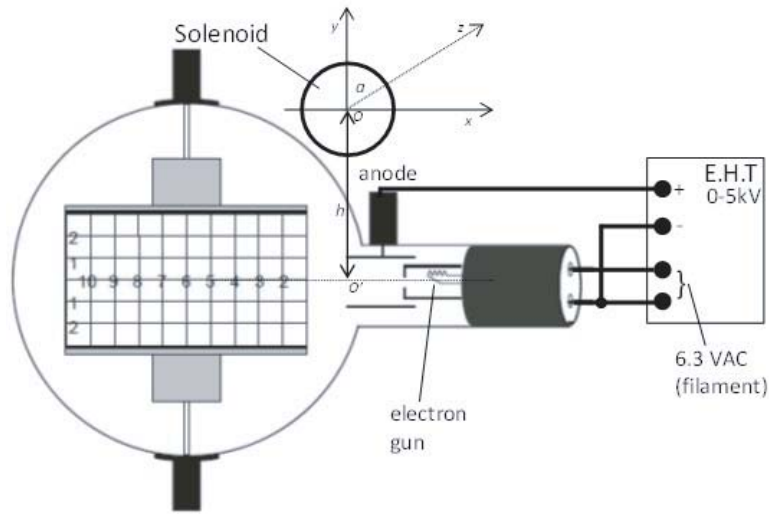
Figure 2. Electron-beam deflection tube with long solenoid positioned centrally above the beam. The exit point, O', of the beam from the electron gun lies in the y-z plane of the solenoid.

at points along the beam and for a given beam velocity, the impulse of the force $\int F_y dt$ can be obtained and hence the vertical momentum change. Then assuming constant mass (non-relativistic) the acquired vertical velocity is calculated and finally the maximum beam deflection (see 3.3.2).

In the computation for the complete solenoid, it is convenient to divide the solenoid into 1 cm sections extending along the z axis. The solenoids employed are double wound and with the same winding density of 26 turns per cm. Then using Eq. (5), F_y is computed for a range of b values (0–10 cm). For a 50 cm solenoid we require,

$$F_y(b) = \frac{2 \times 26 e v I}{4\pi\varepsilon_0 c^2} \sum_{z=0.005}^{0.245} \left[-2ah\left[I_1\right] + 2a^2\left[I_2\right] + \ldots + 3a^3 b\left[I_8\right] \right] \tag{6}$$

where the mean z distances are 0.5, 1.5, 2.5, ..., 24.5 cm and the factor 2 includes both sides of the solenoid. In practice $I = 5.00$ A, $v = 2.06 \times 10^7$ m/s (based on, $v = \sqrt{\frac{2eV}{m_e}}$ where $V = 1200$ V and $e/m_e = 1.76 \times 10^{11}$ C/kg) and the multiplying factor outside the integrand summation is 0.856×10^{-16} (S·I). Numerical computations were carried out using MATLAB utilising trapezium rule with 72 theta steps for b values 0–0.1 m, in steps of 0.002 m.

3.3. Beam Deflection Calculation Based on Lorentz Force Law and Weber-Ritz Force Formula

3.3.1. Lorentz Force Law

Measurement of the external magnetic field close to a long solenoid confirms that, in the vicinity of the electron beam, the field is uniform to within around 10% for the 0.50 and 0.75 m solenoids but not for the 0.25 m length solenoid. Analytical calculations by Farley and Price [8] for long solenoids also validate the uniformity of the field. So the electron beam is subjected to an essentially uniform magnetic field at right angles to its path and the corresponding deflection predicted by the Left Hand Rule. In a uniform magnetic field, **B**, the beam is deflected into a circle of radius, R, producing a vertical deflection, y over a horizontal distance, x. From the geometry of Figure 3, $R^2 = x^2 + (R-y)^2$, making $R = (x^2 + y^2)/2y$. The magnetic component of the Lorentz force law is then equated to the centripetal force, i.e., $Bev = m_e \frac{v^2}{R}$. With the following data values, $v = 2.06 \times 10^7$ m·s^{-1}, $\frac{e}{m_e} = 1.76 \times 10^{11}$ C·kg^{-1} gives,

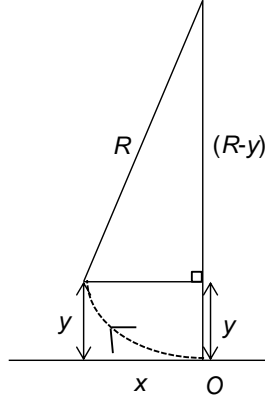$$R = \frac{1.170}{B} \times 10^{-4} \text{ m}$$

Figure 3. e beam deflection in a transverse magnetic field (at right angles to this paper).
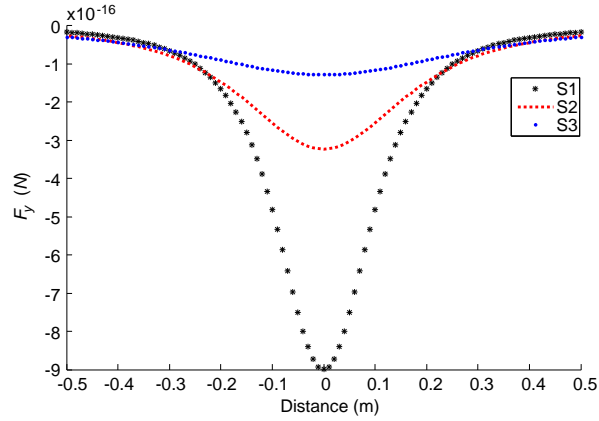

Figure 4. Predicted vertical force variation (Weber-Ritz) for each solenoid as the electron beam approaches and passes. The force is calculated under the assumption that the electron beam is present at each point (i.e., e path does not deviate). The origin represents the plane in which each solenoid would be positioned perpendicular to the approaching e beam and at which the magnitude of the predicted vertical force is greatest.

where the magnetic flux density is given in Tesla. In the actual experiment, $x = 0.10$ m and therefore solving the quadratic in y yields, $y = R \pm \sqrt{R^2 - 0.01}$. Given $R^2 \gg 0.01$, the vertical beam deflection y (mm) over a horizontal distance of 10 cm can be calculated from,

$$y \ (mm) = 0.0427\mathbf{B}$$

where $\mathbf{B}$ is now in µT.

The values of $\mathbf{B}$ for solenoids S1, S2, S3 are obtained from measurements with a Hall probe along the length of the beam. Figure 6 confirms the uniformity of the magnetic field for the solenoids S2 and S3, which is consistent with the calibration graph of Figure 5. However, in the case of solenoid, S1, the non-uniformity of the field makes the calculation of beam deflection uncertain.

3.3.2. Weber-Ritz Force Formula

Computations of the force at various points along the beam using Eq. (6), indicate that across the 10 cm horizontal path the force is non uniform. To account for this non uniformity and to obtain the maximum beam deflection at right angles to the path, the following procedure was adopted. The typical force variation across the beam is represented in Figure 4 where the horizontal axis represents distance (b cm) or time; for a beam velocity of 2.06×10^7 m/s, a 10 cm horizontal travel is traversed in a time interval of 4.85×10^{-9} s.

The impulse, J, given to the electron over 10 cm travel is $\int_0^{4.85 \times 10^{-9}} F_y(b)dt$ is then calculated by simple integration (trap. rule). Impulse is then equated to change of vertical momentum, $J = m_e \times v_v$ where m_e is electron mass and v_v is the final vertical velocity component.

The mean vertical acceleration is then, $a_v = v_v/t$ and the maximum vertical deflection,

$$y \, (\text{max}) = \frac{1}{2} a_v t^2 = \frac{1}{2} v_v t = \frac{1}{2} \left(\frac{J}{m_e} \right) t$$

Now $t = $ time the beam spends in the 10 cm deflection zone $= 4.85 \times 10^{-9}$ s. Finally, the maximum vertical beam deflection in metres is given by, $y = \frac{1}{2}(\frac{J}{m_e}) \times 4.85 \times 10^{-9} = 2.66 \times 10^{21} J$ [m], where J is the calculated impulse [N·s].

4. EXPERIMENTAL INVESTIGATION

The general arrangement is shown in Figure 2. The main feature is a standard Teltron electron beam tube comprising an electron gun which emits a narrow, focussed ribbon of electrons within an evacuated glass bulb. The electron gun is driven by a 5 kV E.H.T unit providing beam velocities of between 2×10^7 and 5×10^7 m/s. An important feature of the tube is that the electron beam is intercepted by a flat mica sheet, one side of which is coated with a fluorescent screen and the other side of which is printed with a centimetre graticule so the electron path is easily traced. The Teltron support stand can accommodate standard Helmholtz coils so electron beam deflections can be calibrated against known transverse magnetic fields.

Three solenoids of lengths 0.25 (S1), 0.50 (S2) and 0.75 (S3) metres, each ~6 cm diameter were used in the investigation. The solenoids are double wound with the same winding density of 2600 turns/metre. A given solenoid is supported between two (non-magnetic) retort stands and positioned centrally across the neck of the beam tube so the central y-z plane of the solenoid coincides with the beam exit for the e gun as shown in Figure 2. Using a series of slim line dc power sources, each solenoid can be provided with a direct current of 5.00 A.

Clearly we are not dealing with 'infinite' solenoids and therefore the external (leakage) field has to be taken into account. It is often repeated that infinite solenoids or toroidal coils carrying direct current have zero external magnetic fields and this is in fact false. Standard electromagnetic theory indicates that in the case of the infinite solenoid there exists an azimuthal field, $B_\emptyset = \mu_0 I/2\pi r$ [9] while for the toroid, there is an r component of the external field which reduces to $B_r = B_z = (\mu_0 I a^2)/2\pi(a^2 + z^2)^{3/2}$ [10] in the neighbourhood of the toroid, z axis; where a is the average radius of the toroid. It is also important to appreciate the sensitivity of the e beam to the presence of relatively small magnetic fields. For example, when the free standing beam tube (gun voltage say 1.5 kV) is rotated sequentially through $360°$ then a maximum beam deflection of around 2 mm is observed with the beam axis aligned in the East-West direction (i.e., at right angles to the Earth's magnetic field, ~20 µT). Experiments were carried out with the beam axis aligned in the North-South direction in order to minimise effects from the Earth's field. There are now three stages to the experimental investigation:-

(1) Given the significance of the axial leakage fields from finite solenoids, it is important to correlate beam deflections with known values of the magnetic field directed at right angles to the beam. This is carried out using the Helmholtz (HH) coils specially adapted for the Teltron beam tube. Given the HH coils provide a uniform magnetic field of close to 4.2 µT/mA, the beam deflection can then be measured for a series of precise direct currents through the coils. This enables a calibration graph of maximum beam deflection (mm) against transverse magnetic field (µT) to be plotted (Figure 5). Such a graph can then be used to check the Lorentz force (magnetic component) on the beam due to the axial magnetic field from the solenoid which crosses the beam at right angles.

(2) The maximum beam deflections are now measured for each of the solenoids in turn. A given solenoid is positioned across the neck of the beam tube and for each case a direct current of 5.00 A is maintained for around 10 seconds. In order to compensate for a residual beam deflection of about 1 mm, in practice the solenoid current is reversed and a mean deflection obtained.

(3) Finally with the beam tube removed the axial magnetic field is measured using a Hall probe at cm locations around each solenoid corresponding to the original beam position (Figure 6). The
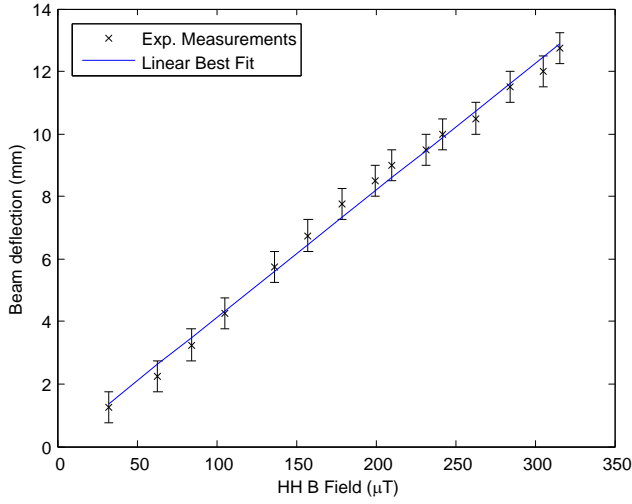
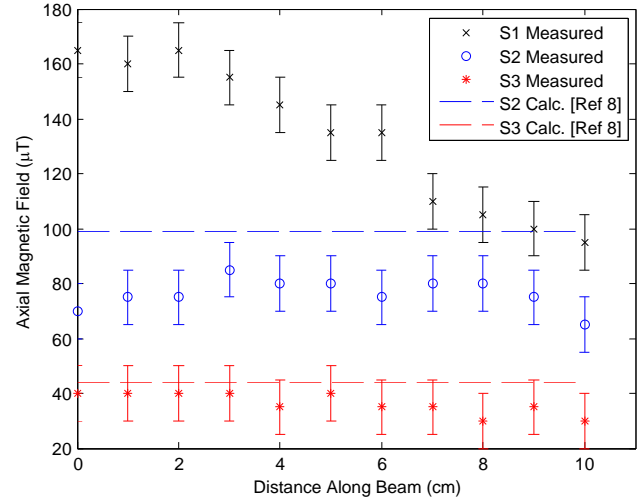**Figure 5.** Measured beam deflection against transverse magnetic field (HH coils at $[4.23I \text{ (mA)}]$ µT).

Figure 6. Magnetic field variation at right angles to electron beam for solenoids S1, S2, S3 with constant d.c current of $5.00\,\text{A}$ applied. Calculated field variations for S2 and S3 are displayed using $B_{ext} = \frac{2}{\pi} \frac{\mu_0 nIA}{L^2}$ [8].
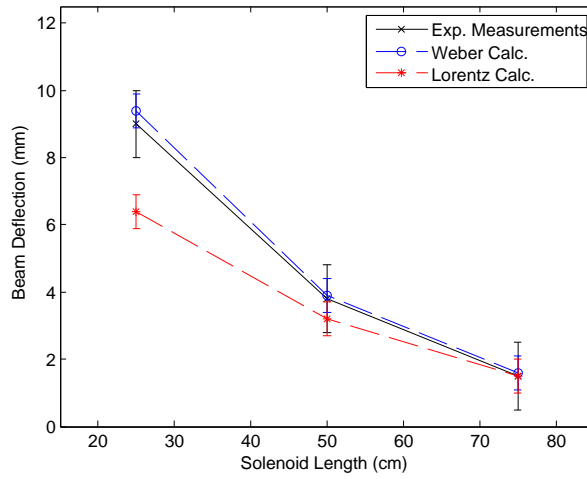

Figure 7. Calculated and measured beam deflections for the three solenoids (S1, S2, S3).

technique is to initially zero the probe; then switch on the solenoid current at $5.00\,\text{A}$ and record the magnetic field in µT; the accuracy was estimated at $\pm 10\,\text{µT}$. Measured values of the axial field for the three solenoids are shown in Figure 6.

5. RESULTS

The results are summarised in Figures 5–7 and Table 1. Figure 5 shows the calibration graph for beam deflections against the transverse magnetic field provided by the HH coils. Figure 6 shows the measured axial (leakage) magnetic fields for the three solenoids used in the experiment. The plots indicate how the external magnetic field from each solenoid varies at points along the electron beam. For the longer solenoids (S2, S3) the field is essentially uniform. This is consistent with the calculated external fields of long solenoids made in [8] where $B(ext) = \frac{2\mu_0 nIr^2}{L^2}$; $n =$ winding density, $r =$ radius, $L =$ length.

Table 1. Summary of calculated and measured beam deflections.

Solenoid Length (m)	Calculated (mm)		Measured (mean, mm)
	Weber-Ritz	Lorentz	
0.25 (S1)	9.4 ± 0.5	6.4 ± 0.5	9.0 ± 1.0
0.50 (S2)	3.9 ± 0.5	3.2 ± 0.5	3.8 ± 1.0
0.75 (S3)	1.6 ± 0.5	1.5 ± 0.5	1.5 ± 1.0

For solenoid S3 carrying a current of 5.00 A, the calculated field is $B \cong 44\,\mu\text{T}$ while for S2, $B \cong 99\,\mu\text{T}$. For the short solenoid S1 such an approximate formula is not valid nor is the uniform field condition. Finally in Figure 5 and Table 1 the essential comparison between experiment and theory is shown. This is illustrated in three plots: (a) the mean measured beam deflections for the three solenoids; (b) the calculated beam deflections based on the Weber-Ritz formula; (c) the calculated beam deflections based on the magnetic component of the Lorentz force law.

The calculation of the maximum beam deflection, based on the Lorentz force law, uses the magnetic flux density of the axial field measured in the vicinity of the electron beam; then the calibration graph of Figure 5 to obtain the beam deflection. However, according to the Lorentz force law the presence of any static electric field will also contribute towards this force. This is now considered.

One source of static electric field will arise from the solenoid self-capacitance becoming charged by the d.c. voltage across the solenoid. Welsby [11] has provided experimental data for single layer solenoid capacitance values. Empirically the self-capacitance in pF is of the same order as the coil diameter in centimetres. So typically for the 75 cm long ×6 cm diameter solenoid, with length/diameter ratio ∼10 the self-capacitance is ∼6 pF. When charged to 80 V, charge accumulated $= Q = 6 \times 10^{-12} \times 80 = 4.8 \times 10^{-10}$ C. Since charge is distributed over 0.75 m, then, $\lambda =$ charge per unit length $= 7.2 \times 10^{-10}$ C/m. Duffin [12] gives the radial **E** field, at radius r from the axis of the cylinder as, $E = \frac{\lambda}{2\pi\varepsilon_0 r}$, and assuming $r = 0.05$ m, this gives an **E** field of around 230 V/m arising from the self-capacitance. Measurement of the radial field at about 2.5 cm from the surface of the same solenoid were also made with an ultra-stable surface d.c. voltmeter (Alpha Labs Inc., USA); the measured values were between 150 and 200 V/m providing reasonable confirmation of the calculation.

The other source of static electric field is that which is a natural consequence of the excess electron charge close to the Earth's surface. Again measurements with the surface d.c. voltmeter indicated a value of around 150 V/m. Now given that, only the component of the **E** field at right angles to the beam is significant, we might expect an overall static **E** field contribution of around 250 V/m. A typical beam deflection calculation in a static field, e.g., Bennet [13] gives, $d = eEl/2\,mv^2$ and so with data, $e/m = 1.76 \times 10^{11}$ C/kg, $E = 250$ V/m, $l =$ length of beam over which field applied $= 0.1$ m, $v = 2.06 \times 10^7$ m/s, gives $d = 0.5$ mm (maximum). In the case of the Earth's field alone we might expect a persistent beam deflection of say about 0.3 mm and this is a likely explanation of the non-zero deflection in the free standing beam tube. Since this is a preliminary investigation our results require to be corroborated by further experimental work involving larger pulses of direct current with a view to reducing error margins.

6. CONCLUDING REMARKS

Our initial investigation of electron beam deflections, by a long direct current carrying solenoid located across the beam, has revealed some interesting results from the stand point of fundamental physics. The Weber-Ritz force formula (involving a series of numerical integrations) applied to calculate electron beam deflections is shown to correlate with the experimental measurements for beam velocities of approx. 2×10^7 m/s. It is emphasised that such a direct action formulation involves only electrical forces between charges. By contrast the field based approach using the Lorentz force formula relies on the measurement of the external **B** fields in the vicinity of the beam, in combination with a calibration graph of beam deflections against known magnetic fields. The magnetic fields for the solenoids S2 and S3 are essentially uniform as predicted in [8], allowing reliable interpolation of beam deflections from the

calibration graph of Figure 5. However, the lack of field uniformity for the case of the shortest solenoid (S1) makes the prediction of the beam deflection unreliable (a mean field value of $150\,\mu\text{T}$ was assumed).

Since the Weber-Ritz force formula relates directly to the electrical forces between moving charges for a discrete system this provides an accurate calculation of electron beam deflection for the smaller solenoid of 25 cm length (S1). In particular, for the solenoid S1 we are able to accurately model the force experienced by the electron beam in a non-uniform (fringing) field. The conventional Maxwell-Lorentz approach relies on the calculation of fields in a continuous system and such an approach is generally complex and computationally intensive [14]. Moreover, Newton's third law is inherently obeyed by Weber's force law and therefore particle momentum and angular momentum are conserved. The results presented in this article are of interest beyond the solenoid-electron beam configuration studied. Our calculations demonstrate the feasibility of using such an approach for modelling charged particle optics in general [15–19].

Although the main concern of the present investigation has been the comparison of Weber-Ritz and Maxwell-Lorentz electrodynamics for this particular case, inevitably the question is raised as to whether a Weber-Ritz type of calculation can provide a possible classical explanation of the AB effect. Boyer [20] has proposed a semi-classical explanation of the AB effect while Batelaan and Tonomura [21], through a combination of experimental and theoretical work, has promoted the quantum mechanical explanation. Boyer has summed up these two points of view, "*. . . currently accepted quantum theory accepts the idea that the electrostatic phase shift of a charge passing a line of electric dipoles is due to a classical lag but claims that the magnetic phase shift of a charge passing a solenoid is due to a new quantum mechanical effect having no classical analogue [20]*".

Moreover, Boyer contends that based on either, (i) the change in kinetic energy of the passing charge through interaction with the constant solenoid current, or, (ii) the acceleration of the solenoid electrons created by the passing electric field of the moving charge; that both should lead to time delays in an electron beam passing a macroscopic solenoid. However, Caprez et al. [22] carried out a time of flight experiment for such a case and found no time delays and therefore concluded that this confirms the absence of forces. In contrast the Weber-Ritz calculation predicts a force based on a constant beam speed (ignoring acceleration terms in the force formula) and for very long solenoids. Further investigation is required working with much smaller diameter solenoids.

It is also appropriate to extend this work in the future, in order to test Weber-Ritz theories for electron velocities approaching light speed. According to O'Rahilly [1, Pages 613–622], for high speed electrons Ritz's theory is consistent with experimental results (and without applying the Lorentz correction factor directly) when the constant λ is assigned the value 3 rather than -1. Such work will require a specially designed beam tube fitted with an electron gun and E.H.T unit providing electron speeds approaching light velocity. This will probably be in the form of a cylindrical tube across which the solenoids can be accurately positioned; the beam deflections can be recorded on a large fluorescent screen at one end of the tube. A direct measurement of beam velocity would be an additional refinement.

REFERENCES

1. O'Rahilly, A., *Electromagnetic Theory: A Critical Examination Of Fundamentals*, Dover Publications, New York, 1965.
2. Smith, R. T., S. Taylor, and S. Maher, "Modelling electromagnetic induction via accelerated electron motion," *Canadian Journal of Physics*, 2014.
3. Assis, A. K. T., *Weber's Electrodynamics*, Springer, 1994.
4. Caluzi, J. J. and A. K. T. Assis, "A critical analysis of Helmholtz's argument against Weber's electrodynamics," *Foundations of Physics*, Vol. 27, 1445–1452, 1997.
5. Assis, A. K. T., W. A. Rodrigues, Jr., and A. J. Mania, "The electric field outside a stationary resistive wire carrying a constant current," *Foundations of Physics*, Vol. 29, 729–753, 1999.
6. Assis, A. K. T., "On the propagation of electromagnetic signals in wires and coaxial cables according to Weber's electrodynamics," *Foundations of Physics*, Vol. 30, 1107–1121, 2000.
7. Kinzer, E. T. and J. Fukai, "Weber's force and Maxwell's equations," *Foundations of Physics Letters*, Vol. 9, 457–461, Oct. 1, 1996.

8. Farley, J. and R. H. Price, "Field just outside a long solenoid," *American Journal of Physics*, Vol. 69, 751–754, 2001.

9. Lorrain, P. and D. R. Corson, *Electromagnetic Fields and Waves*, 2nd edition, W. H. Freeman & Company, New York, 1969.

10. Jackson, J. D., *Classical Electrodynamics*, 2nd edition, J. Wiley & Sons, New York, 1975.

11. Welsby, V. G., *The Theory and Design of Inductance Coils*, Macdonald, 1950.

12. Duffin, W. J., *Electricity and Magnetism*, Volume 3, McGraw-Hill, 1973.

13. Bennet, G. A. G., *Electricity and Modern Physics: Mks Version*, Edward Arnold, 1968.

14. Gibson, J. R., K. G. Evans, S. U. Syed, S. Maher, and S. Taylor, "A method of computing accurate 3D fields of a quadrupole mass filter and their use for prediction of filter behavior," *Journal of the American Society for Mass Spectrometry*, 1–9, 2012.

15. Maher, S., S. U. Syed, D. M. Hughes, J. R. Gibson, and S. Taylor, "Mapping the stability diagram of a quadrupole mass spectrometer with a static transverse magnetic field applied," *Journal of the American Society for Mass Spectrometry*, Vol. 24, 1307–1314, 2013.

16. Maher, S., F. P. Jjunju, and S. Taylor, "Colloquium: 100 years of mass spectrometry: Perspectives and future trends," *Reviews of Modern Physics*, Vol. 87, 113, 2015.

17. Syed, S. U., S. Maher, and S. Taylor, "Quadrupole mass filter operation under the influence of magnetic field," *Journal of Mass Spectrometry*, Vol. 48, 1325–1339, 2013.

18. Syed, S. U., S. Maher, G. B. Eijkel, F. P. M. Jjunju, S. Taylor, and R. M. A. Heeren, "A direct ion imaging approach for the investigation of ion dynamics in multipole ion guides," *Analytical Chemistry*, Vol. 87, 3714–3720, 2015.

19. Satyalakshmi, K. M., A. Olkhovets, M. G. Metzler, C. K. Harnett, D. M. Tanenbaum, and H. G. Craighead, "Charge induced pattern distortion in low energy electron beam lithography," *Journal of Vacuum Science & Technology B*, Vol. 18, 3122–3125, 2000.

20. Boyer, T. H., "Comment on experiments related to the Aharonov-Bohm phase shift," *Foundations of Physics*, Vol. 38, 498–505, 2008.

21. Batelaan, H. and A. Tonomura, "The Aharonov-Bohm effects: Variations on a subtle theme," *Physics Today*, Vol. 62, No. 9, 2009.

22. Caprez, A., B. Barwick, and H. Batelaan, "Macroscopic test of the Aharonov-Bohm effect," *Physical Review Letters*, Vol. 99, 210401, 2007.